# GUIDED MODES IN THE FOUR-LAYER SLAB WAVE-GUIDE CONTAINING CHIRAL NIHILITY CORE

## J.-F. Dong, J. Li, and F.-Q. Yang

Institute of Optical Fiber Communication and Network Technology
Ningbo University, Ningbo 315211, China

**Abstract**—The characteristics of guided modes in the four-layer slab waveguide containing chiral nihility core have been investigated theoretically. The characteristic equation of guided modes is derived. The dispersion curves, energy flux and normalized power of guided modes for three cases of chiral metamaterial parameters are presented. Some abnormal features are found, such as the existence of fundamental mode and surface wave mode, unusual dispersion curves, positive energy flux in the chiral nihility core, and zero power at some normalized frequencies.

## 1. INTRODUCTION

Recently, chiral metamaterials have attracted much attention because the refractive index of a circularly polarized wave in the chiral metamaterial is negative if optical activity is strong enough (the chirality parameter is greater than refraction index) [1–4]. A slab of such chiral metamaterial can be used as a perfect lens which providing subwavelength resolution for circularly polarized waves [5, 6]. In 2009, the effective negative refractive indexes in chiral metamaterials have been realized experimentally at microwave frequencies [7–12] and THz frequencies [13]. Designed and experimental results for chiral metamaterials with negative refractive indexes at infrared frequency have also been published [14–16]. Surface polaritons [17] and Goos-Hänchen shift [18] at the surface of chiral negative refractive media have been studied. Various chiral negative refractive waveguides including chiral metamaterial slab [17, 19, 20], grounded slab [19, 21], parallel-plate [19], fiber [22], have been investigated.

Chiral nihility metamaterial is a special case of chiral negative refractive index medium, in which the permittivity and permeability

are simultaneously zero [1]. The transmission and reflection [23–25], focusing [26], scattering [27, 28] and cloaking [29] properties of the chiral nihility metamaterials have been studied. Fractional dual solutions for chiral nihility metamaterials [30–33] have been discussed. Waves in the parallel-plate waveguide containing two-layer chiral nihility metamaterials and one air layer [34, 35], and in the chiral nihility metamaterial grounded slab [33, 36], circular waveguide [37] have been examined. Such chiral structure can find potential applications in the microwave and millimeter wave integrated circuits [34]. Guided modes and surface wave modes in planar chiral nihility metamaterial waveguides [38, 39] and chiral nihility fibers [40, 41] have been studied in our previous paper. In this paper, we study guided and surface wave modes in the four-layer slab waveguide containing chiral nihility core. Effects of chirality parameter on dispersion curves, energy flux distribution and power are examined and some peculiar characteristics are found. The feature is different from that in the four-layer slab waveguide with left-handed material [42–44].

It is noted that although it is difficult to realize chiral nihility (both permittivity and permeability are zero in the chiral medium), there is another route by magnetoelectric couplings [45, 46] to realize chiral nihility.

## 2. FORMULATIONS

Consider the four-layer slab waveguide containing chiral nihility core whose geometry and material parameters are shown in Fig. 1. The inner layers are an isotropic chiral nihility metamaterial, $\varepsilon_1 = 0$, $\mu_1 = 0, \kappa$, and a conventional dielectric material $\varepsilon_2$, $\mu_2$, the outer layers are conventional dielectric materials $\varepsilon_3$, $\mu_3$ and $\varepsilon_4, \mu_4$. The thickness of the chiral nihility core and inner dielectric layer are $h_1$ and $h_2$, respectively. The outer layers are assumed to extend infinitely.
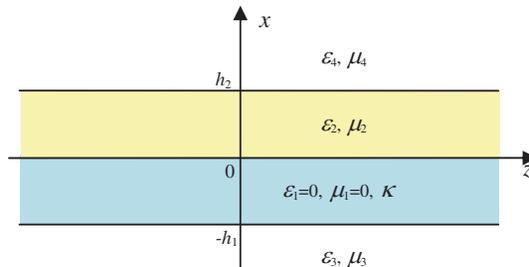


**Figure 1.** Geometry and material parameters of the four-layer slab waveguide containing chiral nihility core.

The constitutive relations in an isotropic chiral nihility metamaterial for a time-harmonic field with $e^{j\omega t}$ are as follows [1]:

$$\mathbf{D} = -j\kappa\sqrt{\mu_0\varepsilon_0}\mathbf{H}, \quad \mathbf{B} = j\kappa\sqrt{\mu_0\varepsilon_0}\mathbf{E} \tag{1}$$

where $\kappa$ is the chirality parameter of the chiral nihility metamaterial.

The electromagnetic fields in the chiral nihility metamaterial can be expressed as [4]:

$$\mathbf{E} = \mathbf{E}_+ + \mathbf{E}_-, \quad \mathbf{H} = \frac{j}{\eta_1}(\mathbf{E}_+ - \mathbf{E}_-) \tag{2}$$

where $\eta_1 = \lim\limits_{\mu_1\to 0,\,\varepsilon_1\to 0}\sqrt{\mu_1/\varepsilon_1}$ is the wave impedance in the chiral nihility metamaterial, and $\mathbf{E}_\pm$ satisfy equations:

$$\nabla \times \mathbf{E}_\pm = \pm k_\pm \mathbf{E}_\pm \tag{3}$$

And then $\mathbf{E}_\pm$ are solutions of the wave equations:

$$(\nabla^2 + k_\pm^2)\mathbf{E}_\pm = 0 \tag{4}$$

where $k_\pm = \pm\kappa k_0$ are the wavenumbers of the two eigenwaves (the subscription $+$ and $-$ correspond to right-handed circularly polarized (RCP) and left-handed circularly polarized (LCP) waves, respectively) in the chiral nihility metamaterial, $k_0 = \omega\sqrt{\mu_0\varepsilon_0}$ is the wavenumber in vacuum. It is obvious that in the chiral nihility metamaterial, LCP eigenwave is a backward wave (here we assume $\kappa > 0$), and the effective refractive index of LCP eigenwave $n_- = k_-/k_0 < 0$.

We can express the solutions of the longitudinal-field component in Equation (4) as:

$$E_{1z+} = Ae^{jk_{1x}x} + Be^{-jk_{1x}x}, \ E_{1z-} = Ce^{jk_{1x}x} + De^{-jk_{1x}x}, \ (-h_1 \le x \le 0) \tag{5}$$

where $e^{j(\omega t - \beta z)}$ is omitted for simplicity and $\beta$ is the longitudinal propagation constant, $k_{1x} = \sqrt{k_1^2 - \beta^2}$, $k_1 = \kappa k_0$, $A, B, C, D$ are constants.

The electromagnetic fields in the conventional dielectric materials also can be expressed as combination of RCP and LCP components, and we express the longitudinal-field components as:

$$E_{2z+} = Ee^{jk_{2x}x} + Fe^{-jk_{2x}x}, \ E_{2z-} = Ge^{jk_{2x}x} + He^{-jk_{2x}x} \ (0 \le x \le h_2) \tag{6}$$

$$E_{3z+} = Ke^{\tau_3(x+h_1)}, \quad E_{3z-} = Le^{\tau_3(x+h_1)} \quad (x \le -h_1) \tag{7}$$

$$E_{4z+} = Me^{-\tau_4(x-h_2)}, \quad E_{4z-} = Ne^{-\tau_4(x-h_2)} \quad (x \ge h_2) \tag{8}$$

where $k_{2x} = \sqrt{k_2^2 - \beta^2}$, $\tau_3 = \sqrt{\beta^2 - k_3^2}$, $\tau_4 = \sqrt{\beta^2 - k_4^2}$, $k_i = n_i k_0$ ($i = 2, 3, 4$), $n_i = \sqrt{\mu_i\varepsilon_i/\mu_0\varepsilon_0}$, $E, F, G, H, K, L, M, N$ are constants.

The relationships between the transversal and longitudinal electromagnetic field components can be found in reference [40]. According to the boundary condition (continuity of the tangential fields) for electromagnetic field components at $x = -h_1$, $0$, $h_2$, the characteristic equation of guided modes can be derived as follow:

$$
\begin{vmatrix}
1 & 1 & 1 & 1 & -1 & -1 & -1 & -1 \\
1 & 1 & -1 & -1 & -\eta_{12} & -\eta_{12} & \eta_{12} & \eta_{12} \\
-\dfrac{k_1}{k_{1x}} & \dfrac{k_1}{k_{1x}} & -\dfrac{k_1}{k_{1x}} & \dfrac{k_1}{k_{1x}} & -\dfrac{k_2}{k_{2x}} & \dfrac{k_2}{k_{2x}} & \dfrac{k_2}{k_{2x}} & -\dfrac{k_2}{k_{2x}} \\
\dfrac{k_1}{k_{1x}} & -\dfrac{k_1}{k_{1x}} & -\dfrac{k_1}{k_{1x}} & \dfrac{k_1}{k_{1x}} & \dfrac{\eta_{12}k_2}{k_{2x}} & -\dfrac{\eta_{12}k_2}{k_{2x}} & \dfrac{\eta_{12}k_2}{k_{2x}} & -\dfrac{\eta_{12}k_2}{k_{2x}} \\
a_{51} & a_{52} & a_{53} & a_{54} & 0 & 0 & 0 & 0 \\
a_{61} & a_{62} & a_{63} & a_{64} & 0 & 0 & 0 & 0 \\
0 & 0 & 0 & 0 & a_{75} & a_{76} & a_{77} & a_{78} \\
0 & 0 & 0 & 0 & a_{85} & a_{86} & a_{87} & a_{88}
\end{vmatrix} = 0 \quad (9)
$$

where

$$
a_{51} = \left( \frac{\eta_{31}k_1}{k_{1x}} - \frac{jk_3}{\tau_3} \right) e^{-jk_{1x}h_1}, \quad a_{52} = -\left( \frac{\eta_{31}k_1}{k_{1x}} + \frac{jk_3}{\tau_3} \right) e^{jk_{1x}h_1},
$$

$$
a_{53} = -\left( \frac{\eta_{31}k_1}{k_{1x}} + \frac{jk_3}{\tau_3} \right) e^{-jk_{1x}h_1}, \quad a_{54} = \left( \frac{\eta_{31}k_1}{k_{1x}} - \frac{jk_3}{\tau_3} \right) e^{jk_{1x}h_1},
$$

$$
a_{61} = -\left( \frac{jk_1}{k_{1x}} + \frac{\eta_{31}k_3}{\tau_3} \right) e^{-jk_{1x}h_1}, \quad a_{62} = \left( \frac{jk_1}{k_{1x}} - \frac{\eta_{31}k_3}{\tau_3} \right) e^{jk_{1x}h_1},
$$

$$
a_{63} = -\left( \frac{jk_1}{k_{1x}} - \frac{\eta_{31}k_3}{\tau_3} \right) e^{-jk_{1x}h_1}, \quad a_{64} = \left( \frac{jk_1}{k_{1x}} + \frac{\eta_{31}k_3}{\tau_3} \right) e^{jk_{1x}h_1},
$$

$$
a_{75} = -\left( \frac{\eta_{42}k_2}{k_{2x}} - \frac{jk_4}{\tau_4} \right) e^{-jk_{2x}h_2}, \quad a_{76} = \left( \frac{\eta_{42}k_2}{k_{2x}} + \frac{jk_4}{\tau_4} \right) e^{jk_{2x}h_2},
$$

$$
a_{77} = a_{75}, \quad a_{78} = a_{76}, \quad a_{85} = \left( \frac{jk_2}{k_{2x}} + \frac{\eta_{42}k_4}{\tau_4} \right) e^{-jk_{2x}h_2},
$$

$$
a_{86} = -\left( \frac{jk_2}{k_{2x}} - \frac{\eta_{42}k_4}{\tau_4} \right) e^{jk_{2x}h_2}, \quad a_{87} = -a_{85}, a_{88} = -a_{86};
$$

and $\eta_{12} = \frac{\eta_1}{\eta_2}$, $\eta_{31} = \frac{\eta_3}{\eta_1}$, $\eta_{42} = \frac{\eta_4}{\eta_2}$, $\eta_i = \sqrt{\mu_i/\varepsilon_i}$ $(i = 2, 3, 4)$.

Energy flux along the $z$-axis in the waveguide is defined by:

$$
S_z = \frac{1}{2}\text{Re}(\mathbf{E} \times \mathbf{H}^*) \cdot \hat{\mathbf{z}} = \frac{1}{2}\text{Re}(E_x H_y^* - E_y H_x^*) \quad (10)
$$

Power in the inner layers ($P_1$, $P_2$) and outer layers ($P_3$, $P_4$) are the

integration of the energy flux:

$$P_1 = \int_{-h_1}^{0} S_{z1} dx dy, \quad P_2 = \int_{0}^{h_2} S_{z2} dx dy,$$

$$P_3 = \int_{-\infty}^{-h_1} S_{z3} dx dy, \quad P_4 = \int_{h_2}^{\infty} S_{z4} dx dy \tag{11}$$

The normalized power is defined as [47]

$$P = \frac{P_1 + P_2 + P_3 + P_4}{|P_1| + |P_2| + |P_3| + |P_4|} \tag{12}$$

## 3. NUMERICAL RESULTS AND DISCUSSION

The longitudinal propagation constant $\beta$ and relationships of constants in the formulas of electromagnetic fields can be calculated numerically from the characteristic equation. Thus all electromagnetic fields components, the energy flow distribution and power can be obtained. In this section, we will present the numerical results for three cases of chiral metamaterial parameters: $\kappa < n_3$, $n_3 < \kappa < n_2$, and $\kappa > n_2$. Here we choose $h_1 = h_2 = h$, $\varepsilon_2 = 2.25\varepsilon_0$, $\varepsilon_3 = \varepsilon_4 = \varepsilon_0$, $\mu_2 = \mu_3 = \mu_4 = \mu_0$ (i.e., $n_2 = 1.5$, $n_3 = n_4 = 1$) and use normalized frequency $k_0 h$ (not frequency) because the chiral nihility metamaterial occurs only at certain frequency.

### 3.1. Case I: $\kappa < n_3$

Figure 2(a) shows the normalized propagation constants (effective refractive index) $n_{eff} = \beta/k_0$ versus normalized frequency $k_0 h$ of guided modes and surface wave mode for $\kappa = 0.5$. There exists fundamental $H_1$ guided mode. The fundamental mode also can exist in four-layer slab waveguide with left-handed material [42, 44] and cannot exist in negative refractive index three slab waveguide [47]. It is noted that guided modes in references [42, 44] are TE mode or TM mode, however, TE (TM) mode cannot be supported in the chiral nihility waveguide, the modes in the chiral nihility waveguide are all hybrid modes, i.e., the electromagnetic fields of modes have both TE and TM components. It is found from Fig. 2(a) that no guided modes can exists in the normalized frequency region between $H_1$ and $H_2$ guided modes. The dispersion curve of $H_1$ guided mode is bent. There are two $n_{eff}$ values for a fixed $k_0 h$ below $k_0 h = 0.4557$ (corresponds to point $A_1$), i.e., appears mode double-degeneracy. As the normalized frequency $k_0 h$ decreases from 0.4557, dispersion curve bifurcate two branches, which $n_{eff}$ increases for upper branch and decreases to $n_{eff} = n_3 = 1$

for lower branch. Dashed curves correspond to $n_{eff} = n_2 = 1.5$, while $n_{eff} > 1.5$, $H_1$ guided mode becomes $H_s$ surface wave mode whose electromagnetic fields exponentially decay on both sides of the interfaces between chiral nihility and conventional materials. The slope of the dispersion curves of $H_1$ guided mode and $H_s$ surface wave mode are very steep, which may have potential application in high-sensitivity optical sensor. Furthermore, the slopes of dispersion curves of upper branch of $H_1$ guided mode and $H_s$ surface wave mode are negative. Consequentially, the normalized power is negative. Fig. 2(c) shows the normalized power $P$ of $H_1$ guided mode and $H_s$ surface wave mode for $\kappa = 0.5$, dispersion curve is also plotted in order to demonstrate clearly (Fig. 2(b)). $P$ is positive for lower branch dispersion curve of $H_1$ guided mode, and negative for $H_s$ surface wave mode. However, the positive value of normalized power is smaller than one, it indicates that the power in the chiral nihility core ($P_1$) is negative for $H_1$ guided mode. For $H_s$ surface wave mode, the power in the chiral nihility core ($P_1$) is negative and its absolute value is greater than total power ($P_2+P_3+P_4$) in inner dielectric layer and outer layers. It is interesting to note that the normalized power $P$ at point $A_1$ equals to zero, corresponding to zero group velocity. It implies that at this point, the waveguide can not propagate energy or it would be able to halt the light. This feature may have potential applications in optical communication and data storage.



(a)                                                                          (b)

                                                                             (c)
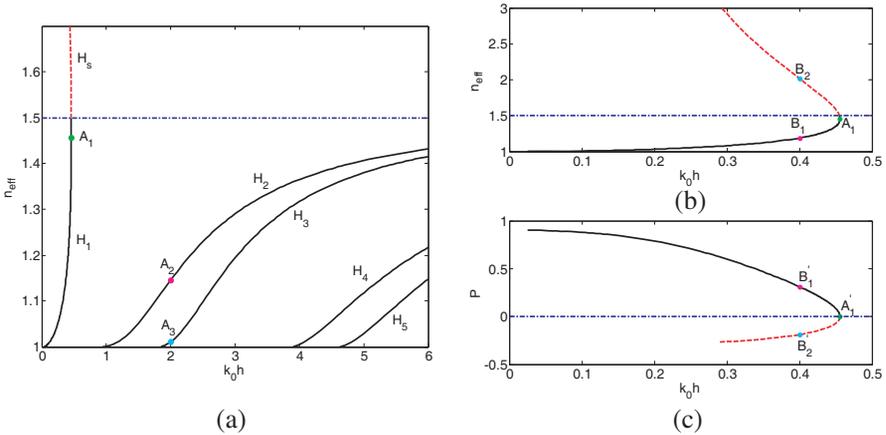
**Figure 2.** (a) Dispersion curves of guided modes and surface wave mode for $\kappa = 0.5$. (b) Dispersion curve and (c) normalized power of $H_1$ guided mode and $H_s$ surface wave mode for $\kappa = 0.5$.

In order to investigate clearly propagation of electromagnetic wave in the waveguide, let's see the energy flux $S_z$ of $H_1$ guided mode and $H_s$ surface wave mode at $k_0 h = 0.4$ (Fig. 3). At point $B_1$ in dispersion curve of $H_1$ guided mode (Fig. 2(b)), $n_{eff} = 1.1890$, $P$ is positive (corresponds to point $B_1'$ in Fig. 2(c)), $S_z$ is negative in chiral nihility core and positive in inner dielectric layer (Fig. 3(a)), it means that the energy flux is in opposite direction in chiral nihility core and inner dielectric layer. However, at point $B_2$ in dispersion curve of $H_s$ surface wave mode (Fig. 2(b)), $n_{eff} = 2.0152$, $P$ is negative (corresponds to point $B_2'$ in Fig. 2(c)), $S_z$ is also negative in chiral nihility core and positive in inner dielectric layer (Fig. 3(b)). $S_z$ always decays exponentially in outer layers, however, $S_z$ of $H_s$ surface wave mode decays more rapidly than that of $H_1$ guided mode, results in $P$ negative for $H_s$ surface wave mode. Thus $H_s$ surface wave mode is a backward wave.



(a) $k_0 h = 0.4$, $n_{eff} = 1.1890$      (b) $k_0 h = 0.4$, $n_{eff} = 2.0152$
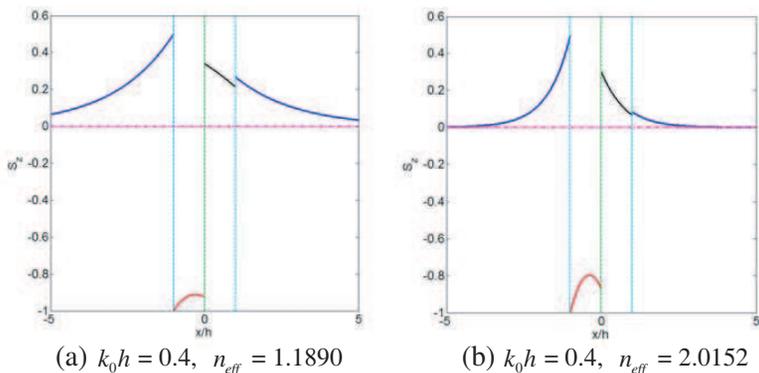
**Figure 3.** Energy flux $S_z$ of $H_1$ guided mode and $H_s$ surface wave mode for $\kappa = 0.5$.

Figure 4 show the energy flux $S_z$ of $H_2$ and $H_3$ guided modes at $k_0 h = 2.0$ for $\kappa = 0.5$ (correspond to $A_2$, $A_3$ in Fig. 2(a), respectively). The energy flux $S_z$ in the chiral nihility core is positive for $H_2$ guided mode and negative for $H_3$ guided mode. Energy flux $S_z$ in the chiral nihility core and inner dielectric layer is in same direction for $H_2$ guided mode and opposite direction for $H_3$ guided mode. The normalized power $P$ equals to 1 for $H_2$ guided mode. Thus $H_2$ guided mode is a forward wave. It is very interesting phenomenon, and has also been found in the chiral nihility fiber [40]. Though the energy flux in chiral nihility core is negative, the normalized power is positive and smaller than one for $H_3$ guided mode because the absolute value of power in the chiral nihility core ($P_1$) is smaller than total power ($P_2 + P_3 + P_4$) in inner dielectric layer and outer layers. The normalized power also

(a) $k_0 h = 2.0$, $n_{eff} = 1.1461$          (b) $k_0 h = 2.0$, $n_{eff} = 1.0112$
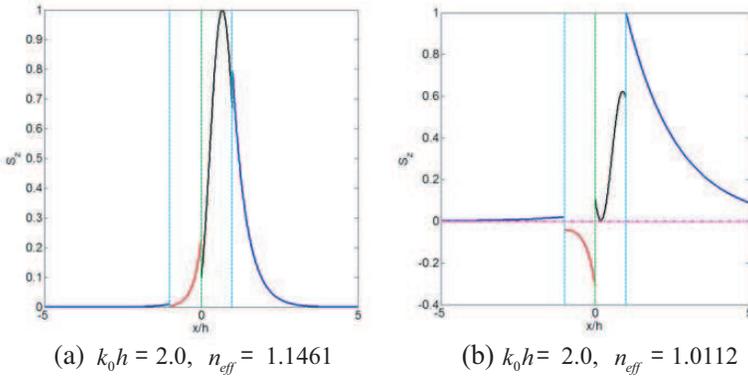
**Figure 4.** Energy flux $S_z$ of $H_2$ and $H_3$ guided modes for $\kappa = 0.5$.

equals to 1 for $H_4$ guided mode and positive (smaller than one) for $H_5$ guided mode. However, $S_z$ has one maximum for $H_2$ and $H_3$ guided modes and two maxima for $H_4$ and $H_5$ guided modes in inner dielectric layer.

## 3.2. Case II: $n_3 < \kappa < n_2$

Figure 5(a) shows the effective refractive index $n_{eff}$ versus normalized frequency $k_0 h$ for guided modes for $\kappa = 1.2$. There also exists fundamental $H_1$ guided mode. $n_{eff}$ of all guided modes increase monotonoically with $k_0 h$. The normalized power $P$ for $H_2$ guided mode is positive, and its value is smaller than one. For all other guided modes, $P = 1$. The energy flux $S_z$ of $H_1$, $H_2$ and $H_3$ guided modes at $k_0 h = 3.0$ for $\kappa = 1.2$ (correspond to points $C_1$, $C_2$, $C_3$ in Fig. 5(a), respectively) are plotted in Figs. 5(b)–(d). Although the difference of $n_{eff}$ values between $H_2$ guide mode (point $C_2$) and $H_3$ guide mode (point $C_3$) is very small, the distribution of energy flux $S_z$ is distinct different. The energy flux $S_z$ in the chiral nihility core is negative for $H_2$ guide mode and positive for $H_3$ guided mode.
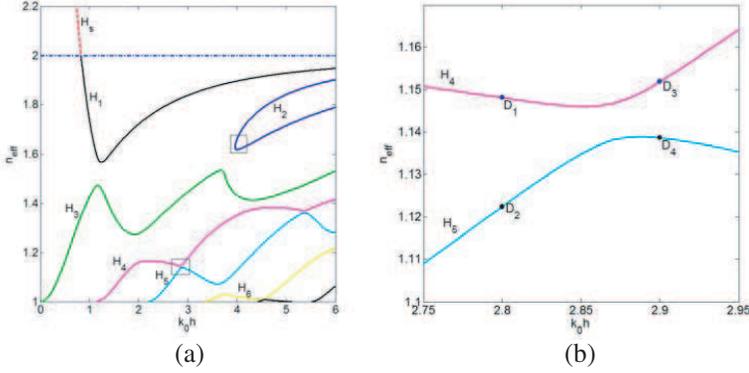
## 3.3. Case III: $\kappa > n_2$

Figure 6(a) shows dispersion curves of guided modes and surface wave mode for $\kappa = 2.0$. The shapes of dispersion curves of guided modes are abnormal and complicated. The fundamental guided mode and surface wave mode also exist. For a fixed higher-order guided mode, there are more than one normalized frequency $k_0 h$ have the same effective refractive index $n_{eff}$. This feature may have potential application in coupling devices.
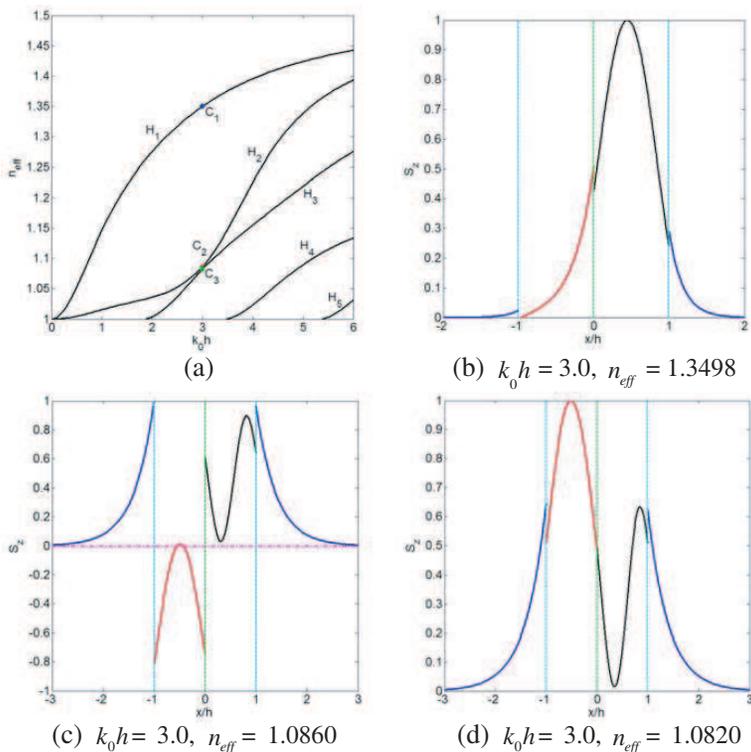
**Figure 5.** (a) Dispersion curves of guided modes for $\kappa = 1.2$. (b) Energy flux $S_z$ of $H_1$, (c) $H_2$ and (d) $H_3$ guided modes for $\kappa = 1.2$.

Figure 7(a) shows normalized power $P$ and dispersion curve of $H_1$ guided mode and $H_s$ surface wave mode. $P$ equals to 1 in the region of positive slope of dispersion curve for $H_1$ guided mode, and $P$ decreases as $k_0 h$ decreases in the region of negative slope of dispersion curve for $H_1$ guided mode and $H_s$ surface wave mode. Fig. 7(b) shows normalized power $P$ and dispersion curve of $H_2$ guided mode. It is strange that $P$ is negative ($F_1' F_2'$ region) for upper branch of dispersion curve ($F_1 F_2$ region) and positive ($F_1' F_3'$) for lower branch of dispersion curve ($F_1 F_3$ region). As $k_0 h$ increases from point $F_3$, $P = 1$.

Generally, for $H_3, H_4, H_5, H_6$ guided modes, in the regions of negative slope of dispersion curves, the energy flux $S_z$ in the chiral nihility core is negative, and $P$ is positive and smaller than one, while in the regions of positive slope of dispersion curves, $S_z$ in the chiral nihility core is positive and $P = 1$. The enlargement of dispersion curves of $H_4$ and $H_5$ guided modes around $k_0 h = 2.85$ are plotted in Fig. 6(b), and the energy flux $S_z$ of $H_4$ and $H_5$ guided modes at
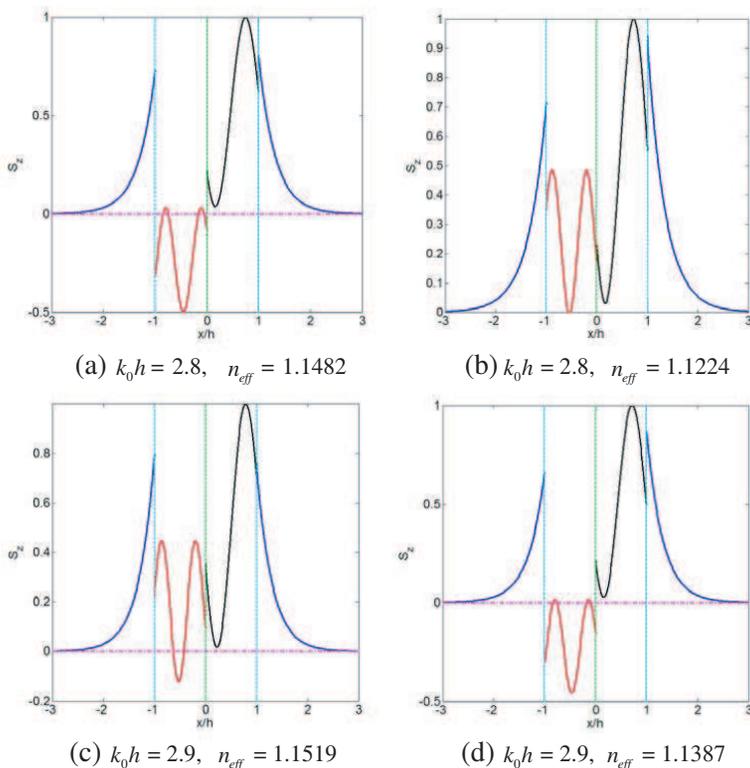
**Figure 6.** (a) Dispersion curves of guided modes and surface wave mode for $\kappa = 2.0$. (b) Dispersion curves of $H_4$ and $H_5$ guided modes around $k_0h = 2.85$ for $\kappa = 2.0$.
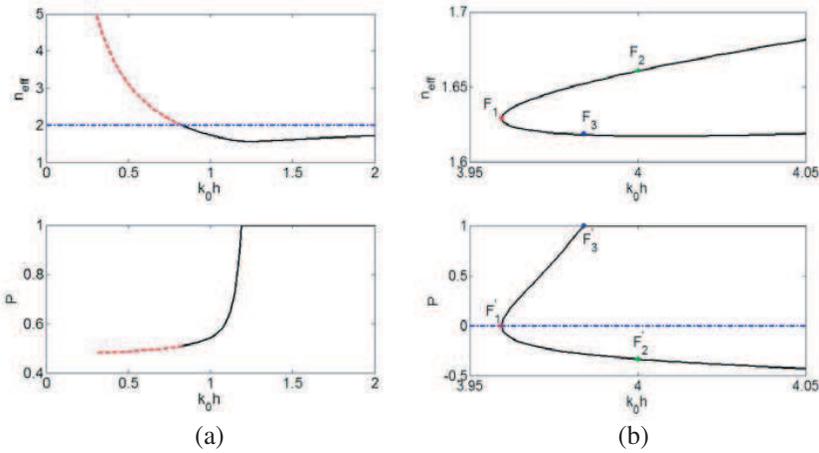


**Figure 7.** (a) Normalized power and dispersion curve of $H_1$ guided mode and $H_s$ surface wave mode, and (b) $H_2$ guided mode for $\kappa = 2.0$.

$k_0h = 2.8$ and $k_0h = 2.9$ are shown in Fig. 8. At $k_0h = 2.8$, $S_z$ in the chiral nihility core is negative (Fig. 8(a)) for $H_4$ guided mode (corresponds to point $D_1$ in Fig. 6(b)) and positive (Fig. 8(b)) for $H_5$ guided mode (corresponds to point $D_2$ in Fig. 6(b)). At $k_0h = 2.9$, $S_z$ in the chiral nihility core is positive (Fig. 8(c)) for $H_4$ guided mode (corresponds to point $D_3$ in Fig. 6(b)) and negative (Fig. 8(d)) for $H_5$ guided mode (corresponds to point $D_4$ in Fig. 6(b)).

(a) $k_0 h = 2.8$, $n_{eff} = 1.1482$     (b) $k_0 h = 2.8$, $n_{eff} = 1.1224$

(c) $k_0 h = 2.9$, $n_{eff} = 1.1519$     (d) $k_0 h = 2.9$, $n_{eff} = 1.1387$

**Figure 8.** Energy flux $S_z$ of $H_4$ and $H_5$ guided modes for $\kappa = 2.0$.

## 4. CONCLUSION

The characteristics of guided and surface wave modes in the four-layer slab waveguide containing chiral nihility core have been investigated theoretically. The characteristic equation of guided modes is obtained. Effects of chirality parameter on dispersion curves, energy flux distribution and power are examined and some peculiar features are found, for examples, the existence of fundamental mode for all chirality parameters, the existence of surface wave mode for smaller and larger chirality parameters, abnormal dispersion curves with different shape, positive energy flux in the chiral nihility core, and zero power at some normalized frequencies. The feature is different from that in four-layer slab waveguide with left-handed material. Guided modes in the chiral nihility waveguide are not TE or TM modes, they are hybrid modes and have both TE and TM components. The results presented here will helpful for potential applications in novel waveguide devices such as directional couplers, high efficient waveguide sensors.

## ACKNOWLEDGMENT

## REFERENCES

1. Tretyakov, S., I. Nefedov, A. Sihvola, S. Maslovski, and C. Simovski, "Waves and energy in chiral nihility," *Journal of Electromagnetic Waves and Applications*, Vol. 17, No. 5, 695–706, 2003.

2. Pendry, J. B., "A chiral route to negative refraction," *Science*, Vol. 306, 1353–1355, 2004.

3. Mackay, T. G., "Plane waves with negative phase velocity in isotropic chiral mediums," *Microwave Opt. Tech. Lett.*, Vol. 45, No. 2, 120–121, 2005.

4. Tretyakov, S., A. Sihvola, and L. Jylhä, "Backward-wave regime and negative refraction in chiral composites," *Photonics and Nanostructures*, Vol. 3, No. 2–3, 107–115, 2005.

5. Monzon, C. and D. W. Forester, "Negative refraction and focusing of circularly polarized waves in optically active media," *Phys. Rev. Lett.*, Vol. 95, 123904, 2005.

6. Jin, Y. and S. He, "Focusing by a slab of chiral medium," *Optics Express*, Vol. 13, No. 13, 4974–4979, 2005.

7. Plum, E., J. Zhou, J. Dong, V. A. Fedotov, T. Koschny, C. M. Soukoulis, and N. I. Zheludev, "Metamaterial with negative index due to chirality," *Phys. Rev. B*, Vol. 79, 035407, 2009.

8. Zhou, J., J. Dong, B. Wang, T. Koschny, M. Kafesaki, and C. M. Soukoulis, "Negative refractive index due to chirality," *Phys. Rev. B*, Vol. 79, 121104 (R), 2009.

9. Wang, B., J. Zhou, T. Koschny, and C. M. Soukoulis, "Nonplanar chiral metamaterials with negative index," *Appl. Phys. Lett.*, Vol. 94, 151112, 2009.

10. Wang, B., J. Zhou, T. Koschny, M. Kafesaki, and C. M. Soukoulis, "Chiral metamaterials: Simulations and experiments," *J. Opt. A: Pure Appl. Opt.*, Vol. 11, 114003, 2009.

11. Wiltshire, M. C. K., J. B. Pendry, and J. V. Hajnal, "Chiral Swiss rolls show a negative refractive index," *J. Phys.: Condens. Matter*, Vol. 21, No. 29, 292201, 2009.

12. Li, Z., R. Zhao, T. Koschny, M. Kafesaki, K. B. Alici, E. Colak, H. Caglayan, E. Ozbay, and C. M. Soukoulis, "Chiral metamaterials with negative refractive index based on four "U" split ring resonators," *Appl. Phys. Lett.*, Vol. 97, 081901, 2010.

13. Zhang, S., Y. Park, J. Li, X. Lu, W. Zhang, and X. Zhang, "Negative refractive index in chiral metamaterials," *Phys. Rev. Lett.*, Vol. 102, 023901, 2009.

14. Kwon, D., D. H. Werner, A. V. Kildishev, and V. M. Shalaev, "Material parameter retrieval procedure for general bi-isotropic metamaterials and its application to optical chiral negative-index metamaterial design," *Optics Express*, Vol. 16, No. 16, 11822–11829, 2008.

15. Dong, J., J. Zhou, T. Koschny, and C. M. Soukoulis, "Bi-layer cross chiral structure with strong optical activity and negative refractive index," *Optics Express*, Vol. 17, No. 16, 14172–14179, 2009.

16. Xiong, X., W. H. Sun, Y. J. Bao, M. Wang, R. W. Peng, C. Sun, X. Lu, J. Shao, Z. F. Li, and N. B. Ming, "Construction of a chiral metamaterial with a U-shaped resonator assembly," *Phys. Rev. B,* Vol. 81, 075119, 2010.

17. Jin, Y., J. He, and S. He, "Surface polaritons and slow propagation related to chiral media supporting backward waves," *Phys. Lett. A*, Vol. 351, No. 4–5, 354–358, 2006.

18. Dong, W., L. Gao, and C.-W. Qiu, "Goos-Hänchen shift at the surface of chiral negative refractive media," *Progress In Electromagnetics Research*, Vol. 90, 255–268, 2009.

19. Dong, J. F., Z. J. Wang, L. L. Wang, and B. Liu. "Novel characteristics of guided modes in chiral negative refraction waveguides," *Proceedings of International Symposium on Biophotonics, Nanophotonics and Metamaterials, Metamaterials 2006*, 517–520, Oct. 2006.

20. Zhang, C. and T. J. Cui, "Chiral planar waveguide for guiding single-mode backward wave," *Opt. Commun.*, Vol. 280, No. 2, 359–363, 2007.

21. Dong, J. F., "Surface wave modes in chiral negative refraction grounded slab waveguides," *Progress In Electromagnetics Research*, Vol. 95, 153–166, 2009.

22. Dong, J. F. and J. Li, "Guided modes in the chiral negative refractive index fiber," *Chinese Optics Letters*, Vol. 8, No. 11 1032–1036, 2010.

23. Qiu, C.-W., N. Burokur, S. Zouhdi, and L.-W. Li, "Chiral nihility

effects on energy flow in chiral materials," *J. Opt. Soc. Am. A*, Vol. 25, No. 1, 55–63, 2008.

24. Tuz, V. R. and C.-W. Qiu, "Semi-infinite chiral nihility photonics: Parametric dependence, wave tunneling and rejection," *Progress In Electromagnetics Research*, Vol. 103, 139–152, 2010.

25. Cheng, X. X., H. S. Chen, B.-I. Wu, and J. A. Kong, "Visualization of negative refraction in chiral nihility media," *IEEE Antennas & Propagation Magazine*, Vol. 51, No. 4, 79–87, 2009.

26. Illahi, A. and Q. A. Naqvi, "Study of focusing of electromagnetic waves reflected by a PEMC backed chiral nihility reflector using Maslov's method," *Journal of Electromagnetic Waves and Applications*, Vol. 23, No. 7, 863–873, 2009.

27. Ahmed, S. and Q. A. Naqvi, "Electromagnetic scattering from a chiral-coated nihility cylinder," *Progress In Electromagnetics Research Letters*, Vol. 18, 41–50, 2010.

28. Ahmed, S. and Q. A. Naqvi, "Directive EM radiation of a line source in the presence of a coated nihility cylinder," *Journal of Electromagnetic Waves and Applications*, Vol. 23, No. 5–6, 761–771, 2009.

29. Cheng, X., H. Chen, X.-M. Zhang, B. Zhang, and B.-I. Wu, "Cloaking a perfectly conducting sphere with rotationally uniaxial nihility media in monostatic radar system," *Progress In Electromagnetics Research*, Vol. 100, 285–298, 2010.

30. Naqvi, Q. A., "Fractional dual solutions to the Maxwell equations in chiral nihility medium," *Opt. Commun.*, Vol. 282, No. 10, 2016–2018, 2009.

31. Naqvi, Q. A., "Fractional dual interface in chiral nihility medium," *Progress In Electromagnetics Research Letters*, Vol. 8, 135–142, 2009.

32. Naqvi, A., S. Ahmed, and Q. A. Naqvi, "Perfect electromagnetic conductor and fractional dual interface placed in a chiral nihility medium," *Journal of Electromagnetic Waves and Applications*, Vol. 24, No. 14–15, 1991–1999, 2010.

33. Naqvi, Q. A., "Fractional dual solutions in grounded chiral nihility slab and their effect on outside field," *Journal of Electromagnetic Waves and Applications*, Vol. 23, No. 5–6, 773–784, 2009.

34. Cheng, Q. and C. Zhang, "Waves in planar waveguide containing chiral nihility metamaterial," *Opt. Commun.*, Vol. 276, No. 2, 317–321, 2007.

35. Naqvi, A., A. Hussain, and Q. A. Naqvi, "Waves in fractional

dual planar waveguides containing chiral nihility metamaterial," *Journal of Electromagnetic Waves and Applications*, Vol. 24, No. 11–12, 1575–1586, 2010.

36. Naqvi, Q. A., "Planar slab of chiral nihility metamaterial backed by fractional dual/PEMC interface," *Progress In Electromagnetics Research*, Vol. 85, 381–391, 2008.

37. Baqir, M. A., A. A. Syed, and Q. A. Naqvi, "Electromagnetic fields in a circular waveguide containing chiral nihility metamaterial," *Progress In Electromagnetics Research M*, Vol. 16, 85–93, 2011.

38. Dong, J. and C. Xu, "Characteristics of guided modes in planar chiral nihility meta-material waveguides," *Progress In Electromagnetics Research B*, Vol. 14, 107–126, 2009.

39. Dong, J. F. and C. Xu, "Surface polaritons in planar chiral nihility metamaterial waveguides," *Opt. Commun.*, Vol. 282, No. 19, 3899–3904, 2009.

40. Dong, J., "Exotic characteristics of power propagation in the chiral nihility fiber," *Progress In Electromagnetics Research*, Vol. 99, 163–178, 2009.

41. Dong, J. F., "Guided and surface modes in chiral nihility fiber," *Opt. Commun.* Vol. 283, No. 4, 532–536, 2010.

42. Zhang, J., Y. He, C. F. Li, and F. M. Zhang, "Guided modes in a four-layer slab waveguide with the LHM core," *Acta Optica Sinica*, Vol. 29, No. 10, 2673–2680, 2009, in Chinese.

43. Tao, F., H. F. Zhang, X. H. Yang, and D. Cao, "Surface plasmon polaritons of the metamaterial four-layered structures," *J. Opt. Soc. Am. B*, Vol. 26, No. 1, 50–59, 2009.

44. Shen, L. and Z. Wang, "Guided modes in a four-layer slab waveguide with dispersive left-handed material," *J. Electromagnetic Analysis & Applications*, Vol. 2, 264–269, 2010.

45. Qiu, C.-W., H.-Y. Yao, L.-W. Li, S. Zouhdi, and T.-S. Yeo, "Backward waves in magnetoelectrically chiral media: Propagation, impedance, and negative refraction," *Phys. Rev. B*, Vol. 75, 155120, 2007.

46. Qiu, C.-W., H.-Y. Yao, L.-W. Li, S. Zouhdi, and T.-S. Yeo, "Routes to left-handed materials by magnetoelectric couplings," *Phys. Rev. B*, Vol. 75, 245214, 2007.

47. Shadrivov, I. V., A. A. Sukhorukov, and Yu. S. Kivshar, "Guided modes in negative-refractive-index waveguides," *Phys. Rev. E*, Vol. 67, 057602, 2003.